B Cell Antigen Receptor Signal Strength and Peripheral B Cell Development are Regulated by a 9-O-Acetyl Sialic Acid Esterase

B cell antigen receptor signal strength and peripheral B cell development are regulated by a 9-*O*-acetyl sialic acid esterase

Annaiah Cariappa,[1] Hiromu Takematsu,[2] Haoyuan Liu,[1] Sandra Diaz,[2] Khaleda Haider,[1] Cristian Boboila,[1] Geetika Kalloo,[1] Michelle Connole,[3] Hai Ning Shi,[1] Nissi Varki,[2] Ajit Varki,[2] and Shiv Pillai[1]

[1]Massachusetts General Hospital, Harvard Medical School, Boston, MA 02129
[2]Glycobiology Research and Training Center, University of California, San Diego, La Jolla, CA 92093
[3]New England Primate Research Center, Harvard Medical School, Southborough, MA 01772

We show that the enzymatic acetylation and deacetylation of a cell surface carbohydrate controls B cell development, signaling, and immunological tolerance. Mice with a mutation in sialate:*O*-acetyl esterase, an enzyme that specifically removes acetyl moieties from the 9-OH position of α2–6-linked sialic acid, exhibit enhanced B cell receptor (BCR) activation, defects in peripheral B cell development, and spontaneously develop antichromatin autoantibodies and glomerular immune complex deposits. The 9-*O*-acetylation state of sialic acid regulates the function of CD22, a Siglec that functions in vivo as an inhibitor of BCR signaling. These results describe a novel catalytic regulator of B cell signaling and underscore the crucial role of inhibitory signaling in the maintenance of immunological tolerance in the B lineage.

CORRESPONDENCE
Shiv Pillai:
pillai@helix.mgh.harvard.edu

Abbreviations used: BCR, B cell receptor; CMAH, CMP-Neu-5Ac hydroxylase; ES, embryonic stem; ITIM, immunoreceptor tyrosine-based inhibitory motif; MZ, marginal zone; MZP, marginal zone B cell precursor; Siae: sialic acid acetyl esterase.

Sialic acids are a diverse family of acidic sugars with a shared nine-carbon backbone. They participate in numerous cell–cell recognition events and can also mediate the binding to vertebrate cells of certain toxins and viruses (1, 2). A relatively common postsynthetic modification of sialic acid is *O*-acetylation at the C-9 position. Acetylation of sialic acid also frequently occurs at the C-7 position, from where the acetyl group can spontaneously migrate to the 9-OH position under physiological conditions. The hemagglutinin esterases of influenza C viruses and certain nidoviruses, including group 2 coronaviruses, recognize 9-*O*-acetylated sialic acid–containing glycoconjugates on the surface of host cells, and some can remove the 9-*O*-acetyl moieties (3, 4). However, the in vivo biological function of this acetylation event has remained a mystery. One attempt to elucidate the biological role of sialic acid 9-*O*-acetylation involved the transgenic expression of Influenza C hemagglutinin esterase in mice (5). This led to a defect in early embryogenesis, indirectly suggesting that 9-*O*-acetyl sialic acid may be essential during murine development. In vitro studies (6) suggested that 9-*O*-acetylation of α2–6-linked sialic acid containing glycoconjugates impairs the recognition of this glycan moiety by certain Siglecs (sialic acid binding Ig superfamily lectins) including CD22. However, despite these and other tantalizing clues, the intrinsic in vivo functions of this abundant modification have not been established.

The Siglecs are the largest known group of vertebrate sialic acid-recognizing cell surface proteins. This family comprises 13 members in humans including sialoadhesin (Siglec-1), CD22 (Siglec-2), CD33 (Siglec-3), myelin associated glycoprotein (Siglec-4), Siglec-15, and the so-called CD33-related Siglecs, 5–10, 11, and 14 (7–9). CD22 is one of the best studied Siglecs and binds specifically to α2–6-linked sialic acid–containing N-glycans (10, 11). CD22 inhibitory signaling depends on the recruitment of SHP-1 to phosphorylated tyrosine residues in immunoreceptor tyrosine-based inhibitory motifs (ITIM) in its cytoplasmic tail (12).

H. Takematsu's present address is Laboratory of Membrane Biochemistry and Biophysics, Graduate School of Biostudies, Kyoto University, Kyoto 606-8501, Japan.

The Rockefeller University Press $30.00
J. Exp. Med. Vol. 206 No. 1 125-138
www.jem.org/cgi/doi/10.1084/jem.20081399

The Journal of Experimental Medicine

Antigen receptor cross-linking leads to the activation of Lyn and other less abundant Src-family kinases that phosphorylate ITIM tyrosines in CD22. Initiation of inhibitory signaling by CD22 is not well understood and the exact mechanism remains controversial. The simplest model that may be indirectly inferred from the phenotypes of KO mice (13–20) suggests that antigen receptor ligation contributes to the sialic acid–dependent recruitment of CD22 to the BCR and the subsequent phosphorylation by Lyn of CD22 ITIM tyrosines, which is followed by the recruitment and activation of SHP-1. Other mechanisms of signal initiation have been suggested by several studies variously implicating sialic acid–dependent homooligomerization and sialic acid–independent association of this Siglec with the B cell receptor (BCR) (21–24). Because CD22 is expressed constitutively on mature B cells and α2–6-linked sialic acid–containing *N*-glycans are abundantly present on the cell surface, it could be argued that CD22 inhibition may itself be constitutive. How inhibitory signaling via CD22 is temporally regulated in mature B cells is unclear. Because CD22 does not bind to 9-*O*-acetylated sialic acid in vitro (6), we considered the possibility that the function of this Siglec might be regulated in vivo by the enzymatic acetylation and deacetylation of α2–6-linked sialic acid. Sialic acid acetyl esterase (Siae), which is molecularly characterized as an enzyme that removes acetyl groups from the 9-OH position of α2–6-linked sialic acid (25), was also independently identified as a gene that is up-regulated during B cell maturation (26), suggesting a role in the biology of B lymphocytes. In this paper, we show that Siae influences B cell signaling and B cell development and participates in inhibitory signaling mechanisms that are crucial to the maintenance of immunological tolerance in the B lineage.

RESULTS

Sialate *O*-acetylesterase is secreted and can access the cell surface

The *Siae* gene (*sialate:O-acetyl esterase*) can generate two alternatively spliced variants. One form contains a signal peptide and can encode a protein that enters the secretory pathway (originally called Lse [lysosomal sialic acid acetylesterase]), whereas the other lacks this signal peptide and encodes a cytosolic esterase (25–27). Although the Lse protein was thought to localize to lysosomes, a site that would not be suitable for the modification of Siglec ligands, we have observed in transfected cells that this protein exhibits, at best, a limited lysosomal localization and is secreted and can bind to the surface of transfected cells (Figs. S1 and S2, available at http://www.jem.org/cgi/content/full/jem.20081399/DC1). The enzyme, therefore, has the potential to remove acetyl groups from 9-*O*-acetylated Siglec ligands in a post Golgi vesicle or at the cell surface. Although some antibodies against Siae have been generated, they lack the specificity to detect Siae in murine cells and tissue sections. The actual location of the Siae protein in murine B cells is therefore yet to be conclusively established.

Generation of *Siae*$^{\Delta 2/\Delta 2}$ mice

Exon 2 of the *Siae* gene is unique to *Lse*. An engineered in-frame deletion of exon 2 in a murine *Lse* complementary DNA resulted in a protein that lacked esterase activity (Fig. 1 A). Genomic deletion of exon 2 was achieved as described in the Materials and methods (Fig. 1 B). After germline transmission, homozygous mutant mice were generated and were found to be viable. Truncated exon 2–deficient *Siae* mRNA could be detected in KO mice (Fig. S3, available at http://www.jem.org/cgi/content/full/jem.20081399/DC1). Cytosolic esterase mRNA continues to be transcribed in these mutant mice. We refer to these KO animals as *Siae*$^{\Delta 2/\Delta 2}$ mice.

Enhanced B lymphocyte antigen receptor signaling in *Siae*$^{\Delta 2/\Delta 2}$ mice

Because Siae has the potential to remove 9-*O*-acetyl residues from α2–6-linked sialic acid containing Siglec ligands, we predicted that B cells from mice lacking this esterase might exhibit enhanced BCR signaling similar to that noted in CD22-null mice (13–16). Mice were first bred into the C57BL/6 background for 10 generations. B cells from WT and *Siae*$^{\Delta 2/\Delta 2}$ mice were gated on, and the accumulation of cytoplasmic calcium after ligation of the BCR was analyzed using flow cytometry. As seen in Fig. 2, BCR cross-linking resulted in an accelerated and enhanced calcium flux. A similar result was seen when purified splenic B cells from mutant and WT mice were analyzed (Fig. S4, available at http://www.jem.org/cgi/content/full/jem.20081399/DC1). These data suggested that in the absence of functional Siae, BCR signal strength is markedly enhanced and that this alteration in signal strength is an intrinsic property of mutant B lymphocytes.

Defective CD22 signaling and hyperacetylation of α2–6-linked sialic acid moieties on *Siae* mutant B cells

The defect in Siae could result in the increased acetylation of α2–6-linked sialic acid on *N*-glycans in B cells and, thus, attenuate the ability of glycoproteins on B cells to ligate CD22 and generate inhibitory signals. We sought to examine if there was a defect in CD22 signaling in *Siae*$^{\Delta 2/\Delta 2}$ mice. After BCR cross-linking, CD22 was isolated by immunoprecipitation, and immunoprecipitates were examined for CD22 tyrosine phosphorylation and for associated SHP-1 using Western blot assays. As seen in Fig. 3 (left, experiment 1; and right, experiment 2), tyrosine phosphorylation of CD22 after BCR signaling was reduced in *Siae*$^{\Delta 2/\Delta 2}$ mice in spite of similar levels of surface CD22 expression in WT and mutant mice (Figs. S5 and S6, available at http://www.jem.org/cgi/content/full/jem.20081399/DC1). Recruitment of SHP-1 by CD22 was clearly impaired after BCR ligation of *Siae*$^{\Delta 2/\Delta 2}$ B cells as compared with WT B cells. This result showing diminished SHP-1 recruitment in *Siae*$^{\Delta 2/\Delta 2}$ B cells is consistent with the accelerated enhancement in BCR signal strength observed in *Siae*$^{\Delta 2/\Delta 2}$ mice.

It remained to be demonstrated whether a defect in Siae would result in enhanced 9-*O*-acetylation of α2–6-linked sialic acid in *Siae*$^{\Delta 2/\Delta 2}$ mice. 9-*O*-acetylation of sialic acid has not

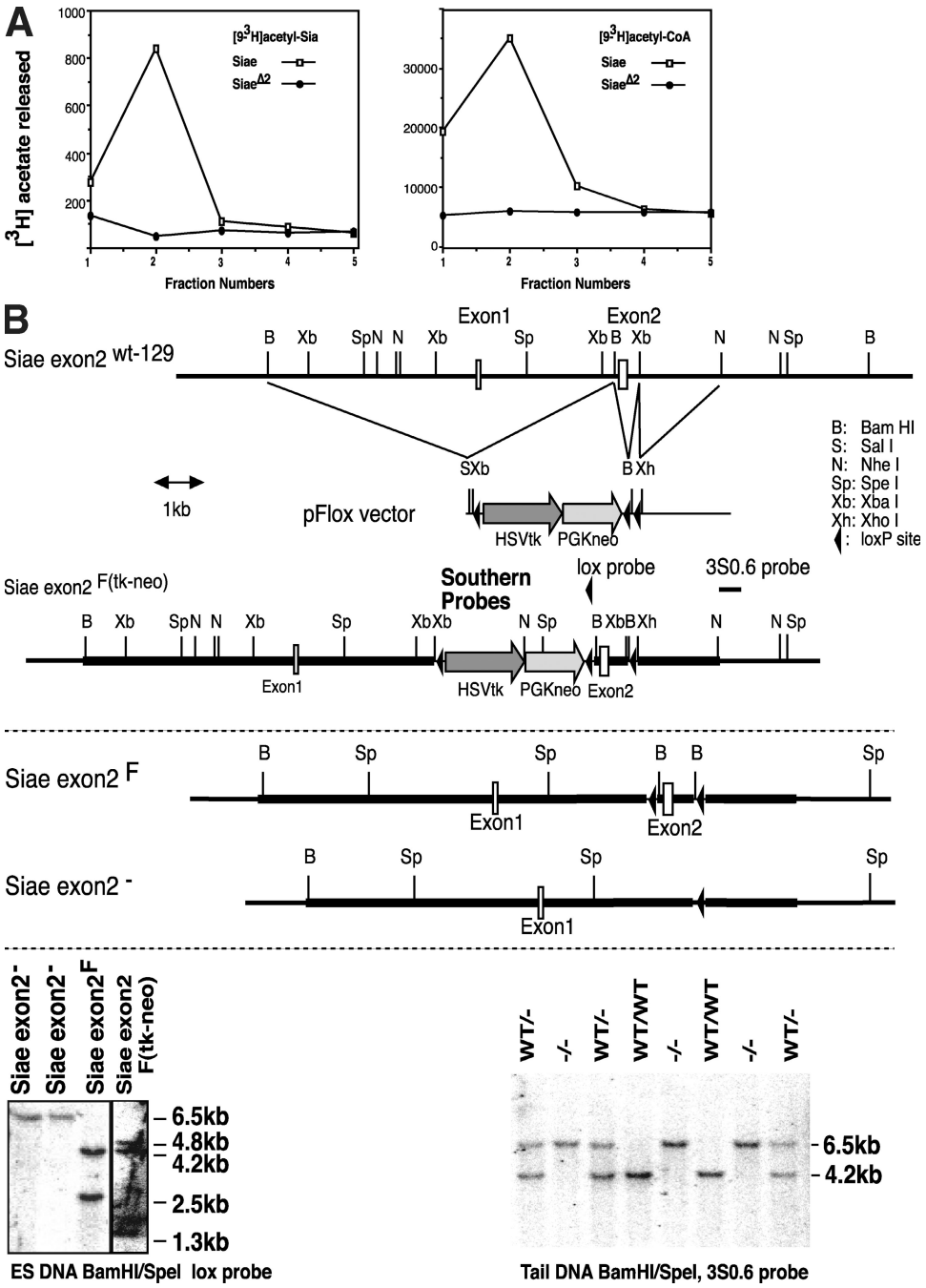

Figure 1. Targeted deletion of exon 2 of murine *Siae* results in enhanced BCR signaling. (A) Deletion of exon 2 abrogates the esterase activity of the Lse form of Siae. A WT C-terminal FLAG-tagged murine *Siae* expression construct of the *Lse* form and an exon 2–deleted version of this complementary DNA were transfected into COS7 cells. Cell culture medium was recovered and the recombinant protein purified by an antibody column directed to the FLAG epitope. Western blotting analysis on eluate fractions showed that both proteins were expressed, bound, and eluted from the column. Column eluate fractions were subjected to an assay for sialic acid 9-*O*-acetylesterase activity (left) and acetyl-CoA esterase activity (right) as previously described (25). Y axes show cpm. (B) Targeting strategy for the deletion of exon 2 of murine Siae. The top shows the targeting construct used to specifically target exon 2 of *Siae*. The middle shows the expected structure of the locus after targeting. The bottom left shows Southern Blotting of embryonic stem (ES) cells at each step of manipulation detected by a loxP-specific probe. The black line indicates that intervening lanes have been spliced out. The bottom right shows Southern blotting of mouse tail DNA after mating heterozygous mice that also expressed the ZP3-Cre Transgene. The expected deleted fragment is 6.5 kb and the expected WT fragment is 4.2 kb.

been previously observed on B cells, and it is likely that this modification occurs only transiently on WT B lymphocytes. A well established reagent for the detection of 9-*O*-acetylated α2–6-linked sialic acid is a fusion protein containing the Fc portion of human IgG and the influenza C hemagglutinin esterase treated with diisopropyl fluorophosphate (28). Modification of the catalytic serine nucleophile in this fusion protein by diisopropyl fluorophosphate permits the viral protein to bind to 9-*O*-acetyl sialic acid but not to cleave it. This reagent, designated CHE-FcD, binds to *N*-linked glycans that are decorated with 9-*O*-acetylated α2–6-linked sialic acid moieties. As predicted, a consistent increase in 9-*O*-acetylation was detected in *Siae*$^{\Delta 2/\Delta 2}$ B cells compared with WT B cells (Fig. 4).

In keeping with the increased magnitude of BCR signaling, antigen receptor ligation induced enhanced proliferation of B cells in *Siae*$^{\Delta 2/\Delta 2}$ mice (Fig. S7, available at http://www.jem.org/cgi/content/full/jem.20081399/DC1). Thymidine uptake studies uncovered a delayed stimulus strength–dependent inhibition of proliferation (Fig. S8) that might be related to a modest increase in ongoing spontaneous apoptosis of follicular B cells in mutant mice (Fig. S9). Four different CD22-null mutant mice have been described by different groups (13–16), and although enhanced antigen receptor signaling was observed in all four mutants, BCR-induced proliferation was enhanced in some mutants and diminished in others. Enhanced cell death has also been reported in some CD22 mutants (14, 16).

Siae influences peripheral B cell development

Enhanced BCR signaling in the absence of negative regulators of the BCR such as Aiolos or CD22 has been linked to the relative absence of marginal zone (MZ) B cells (29–31). As seen in Fig. 5 A, immunohistochemistry revealed a marked reduction in splenic MZ B cells in *Siae*$^{\Delta 2/\Delta 2}$ mice, although

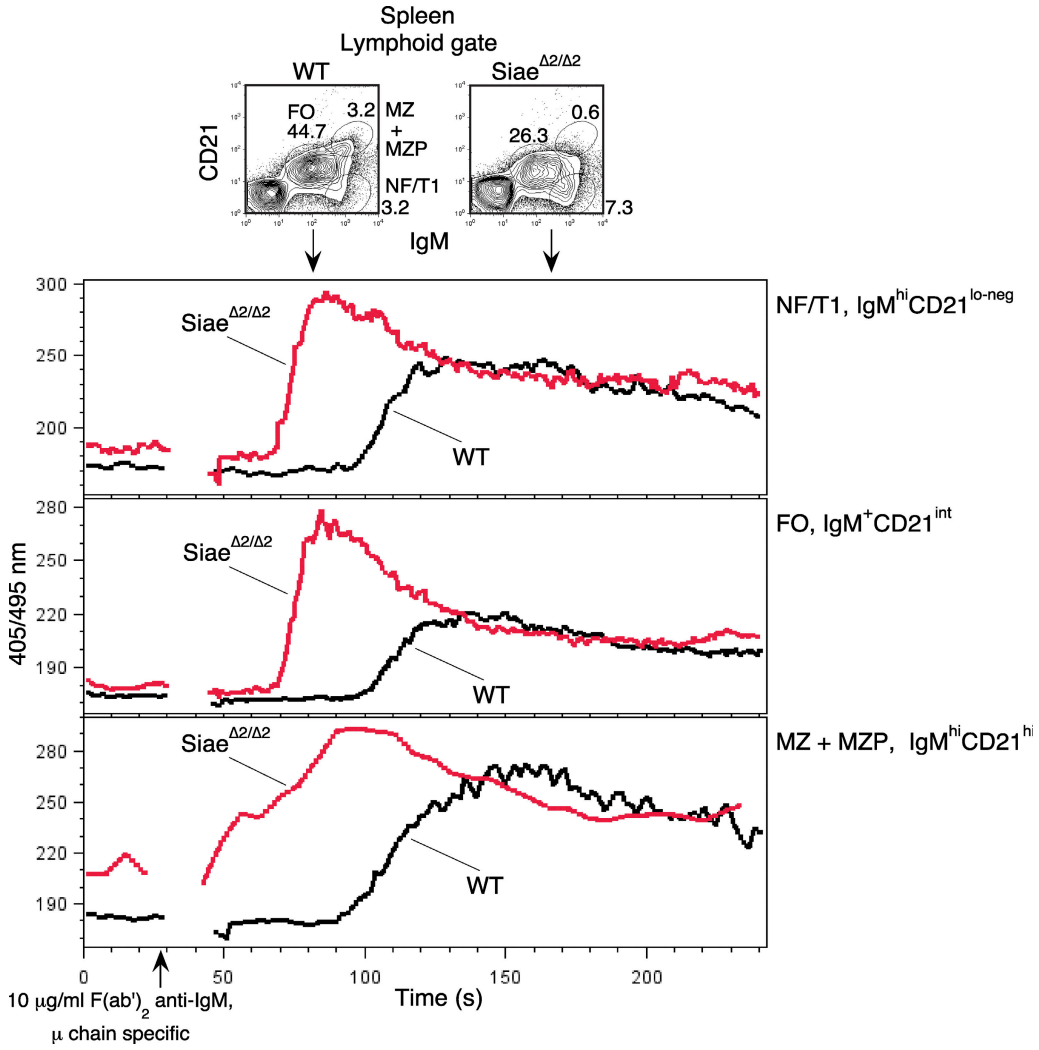

Figure 2. Accelerated and enhanced BCR signaling in Siae mutant mice. Splenocytes from mutant and WT mice were loaded with Indo-1, reacted with 2.4G2, an Fcγ III/II receptor-blocking antibody, stained with follicular and MZ B cell phenotype markers, and stimulated with F(ab′)$_2$ anti-IgM. Populations gated on include newly formed (NF/T1), follicular (FO), and MZ B cells and their precursors (MZ and MZP). Results are representative of three separate experiments and a total of six mice.

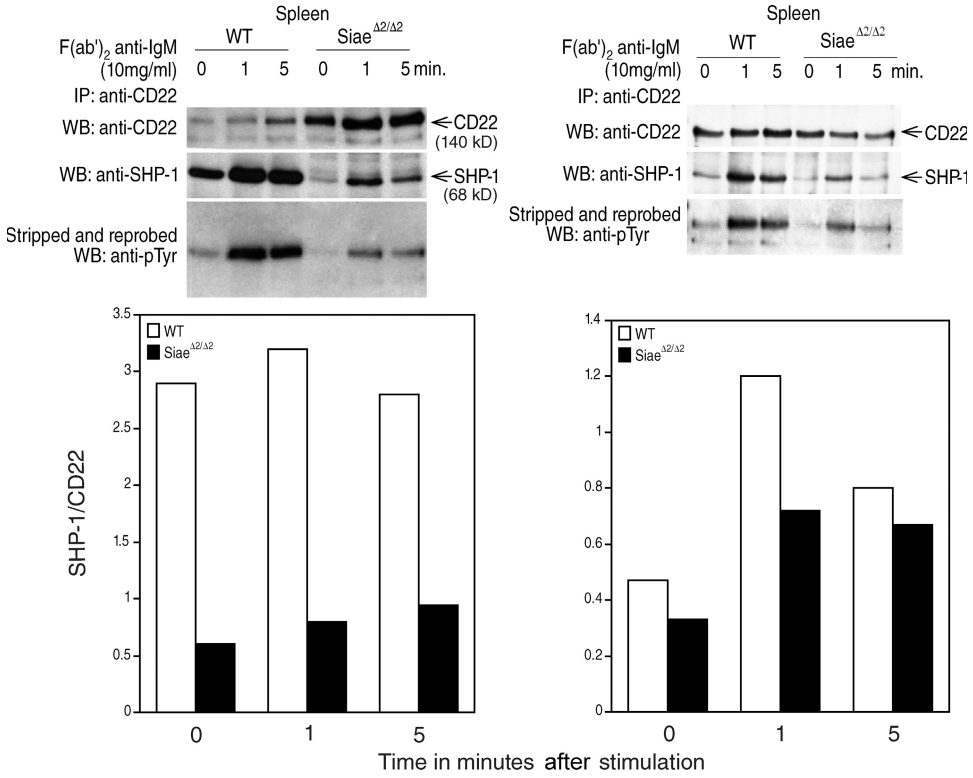

Figure 3. Defective CD22 signaling in *Siae*$^{\Delta2/\Delta2}$ mice. Decreased recruitment of SHP-1 by CD22 in Siae mutant mice. Splenocytes from mutant and WT mice were stimulated via the BCR and immunoprecipitated with antibody to CD22, and Western blots were developed with antibodies to SHP-1, CD22, and phosphotyrosine. Results of two experiments are shown on the top left and the top right. The bottom presents SHP-1/CD22 ratios quantitated by densitometry.

some reduction in follicle size was also apparent. Flow cytometric analysis revealed that IgM^{hi}IgD^{hi} CD21^{hi} MZ B cell precursors (MZP), as well as IgM^{hi}IgD^{lo}CD21^{hi} MZ B cells, were markedly reduced in *Siae*$^{\Delta2/\Delta2}$ mice (Fig. 5 B). An analysis of the absolute numbers of B cells in *Siae*$^{\Delta2/\Delta2}$ mice (Table I) revealed a striking decrease in MZP and MZ B cells and a more modest reduction in follicular B cells. These results are consistent with the ability of Siae to negatively regulate BCR signaling.

Follicular B cells occupy two niches: the follicular niche in conventional secondary lymphoid organs and the perisinusoidal niche in the BM (32, 33). In mutant mice, including *Aiolos*$^{-/-}$ mice, *CD22*$^{-/-}$ mice, and *CD72*$^{-/-}$ mice, all of which exhibit enhanced BCR signal strength, there is

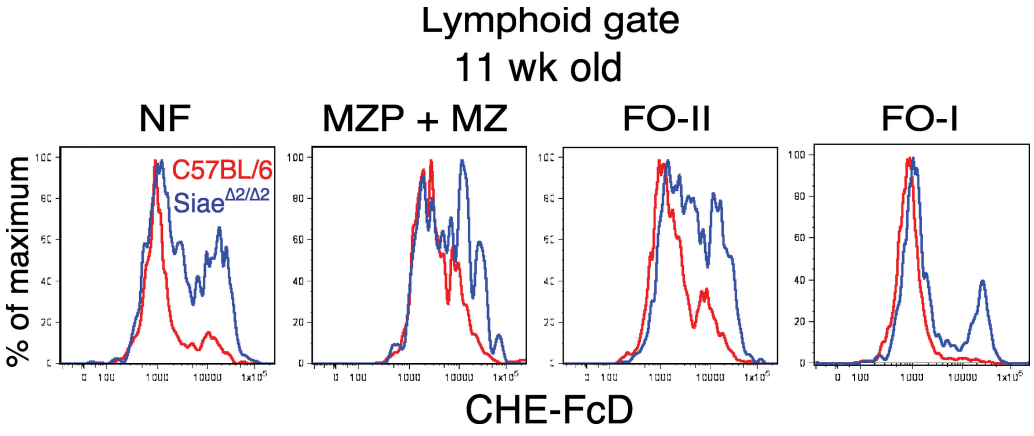

Figure 4. Increased 9-*O*-acetylation of α2–6-linked sialic acid in Siae mutant B cells. Splenocytes from 11-wk-old WT and mutant mice were treated with the CHE-FcD reagent and stained with surface phenotype markers. Results are representative of three mice. X axes show log of fluorescence intensity.

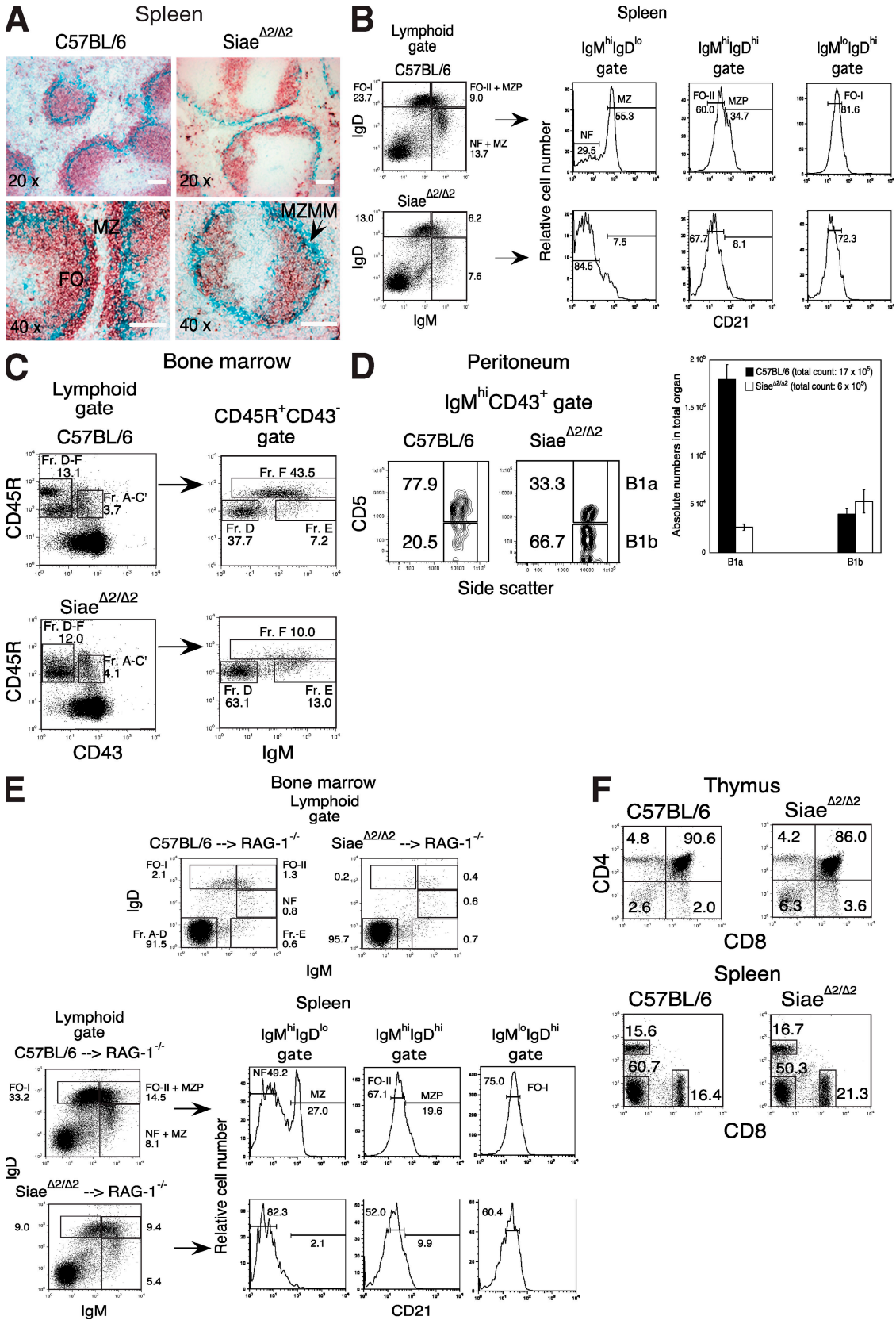

Figure 5. The *Siae* mutation affects the development of MZ and perisinusoidal B cells in a cell-intrinsic manner. (A) Immunohistochemistry reveals a decrease in MZ B cells in *Siae*$^{\Delta 2/\Delta 2}$ spleens. B cells were stained with anti-IgM (brown) and metallophilic macrophages with the MOMA-1

a selective loss of recirculating follicular phenotype B cells from the perisinusoidal niche even as these cells efficiently seed the follicular niche (14–16, 34, 35). We examined follicular phenotype B cell populations in the perisinusoidal niche in *Siae*$^{\Delta 2/\Delta 2}$ mice and noted a marked and selective loss of recirculating B cells in the BM (Fig. 5 C and Table II, fraction F), again paralleling a phenotypic alteration previously noted in CD22-null mice (14–16). We analyzed peritoneal B-1 B cell populations in *Siae*$^{\Delta 2/\Delta 2}$ and WT mice and noted an increase in IgM^{hi} CD43^{+} CD5^{-} B1b B cells but decreased numbers of IgM^{hi} CD5^{+} B1a B cells in *Siae*$^{\Delta 2/\Delta 2}$ mice (Fig. 5 D). The CD22 mutants showed increased B1 cells (13), increased B1a cells (15), or normal numbers (16).

A lymphocyte-intrinsic defect in Siae contributes to peripheral B cell phenotypes

To determine whether the alteration in peripheral B cell populations reflected a cell-intrinsic defect in Siae function, we reconstituted *Rag-1*$^{-/-}$ mice with hematopoietic stem cells from WT and *Siae*$^{\Delta 2/\Delta 2}$ BM. *Siae*$^{\Delta 2/\Delta 2}$ lymphocytes in reconstituted mice exhibited a defect in MZ B cell development and a reduction of perisinusoidal BM B cells (Fig. 5 E), which establishes that these developmental abnormalities represent lymphocyte-intrinsic defects. No gross defect in T cell development was discovered in the absence of Siae (Fig. 5 F), although there was a small decrease in T cell numbers both in the thymus and the spleen (Tables III and IV). Other B cell–deficient mice have been reported to have a mild decrease in T cell numbers (36). The phenotype of *Siae* mutant mice in which a subtle alteration may have been generated in CD22 ligands is very different from that of the *ST6GalI*-null mouse, which completely lacks α2–6-linked sialic acid and which presents with defects in B cell activation and in thymocyte development (37, 38). Murine CD22, unlike human CD22, has a markedly higher affinity for Neu5Gc (sialic acid with an *N*-glycolyl moiety in the C5 position; the major form in the mouse) as compared with Neu5Ac (sialic acid with an *N*-acetyl moiety in the C5 position) (39–42). The enzyme CMP-Neu-5Ac hydroxylase (CMAH) converts CMP-Neu5Ac to CMP-Neu5Gc, and mice lacking this enzyme not only synthesize *N*-glycans with a subtly different form of sialic acid that binds CD22 poorly but they also exhibit a poorly understood down-regulation of *Siae* expression and an increase in 9-*O*-acetylation of Neu5Ac (43). *Cmah*-null mice as well as *Cmah*/*Siae* double mutant mice would therefore be expected to exhibit BCR hyperreactivity, the relative loss of MZ B cells, and a relative loss of perisinusoidal B cells. Indeed, B cells from *Cmah* mutant mice have been reported to exhibit an enhanced proliferative response to BCR cross-linking (44). We show here that B cells from *Cmah*-null mice have higher levels of 9-*O*-acetyated sialic acid as revealed by CHE-FcD binding (Fig. S10, available at http://www.jem.org/cgi/content/full/jem.20081399/DC1). Both *Cmah*-null mice and *Cmah*/*Siae* double mutant mice present with enhanced BCR activation as measured by the release of intracellular calcium after antigen receptor ligation and, as predicted, present with marked reductions in MZ B cells and perisinusoidal B cells (Figs. S10 and S11). A combination of two changes in the structure of sialic acid that each compromise CD22 binding results in a phenotype that is similar to that seen in mice with enhanced 9-*O*-acetylation of sialic acid alone but is quite distinct from the phenotype of mice with the complete loss of α2–6-linked sialic acid.

Siae mutant mice exhibit spontaneous increases in class-switched immunoglobulins and autoantibodies

Many phenotypic features of *Siae*$^{\Delta 2/\Delta 2}$ mice resemble those seen in the absence of CD22. These include enhanced BCR signaling, the loss of MZ B cells, and a reduction in perisinusoidal B cells. Subtle alterations in responses to synthetic T-dependent and T-independent antigens have been described in CD22-null mice, and an altered spectrum of responsiveness to similar antigens was also noted in *Siae*$^{\Delta 2/\Delta 2}$ mice. Immunization with DNP-KLH resulted in diminished IgG2a, IgG2b, and IgG3 responses in *Siae* mutant mice (Fig. S12, available at http://www.jem.org/cgi/content/full/jem.20081399/DC1). *Siae*$^{\Delta 2/\Delta 2}$ mice spontaneously developed high levels of certain class-switched serum immunoglobulins, including IgE and IgG$_{2b}$ (Fig. 6 A), as well as high titers of antinuclear antibodies and circulating immune complexes as early as at 20 wk of age (Fig. 6 B). These mice also develop an immune complex glomerulonephritis (Fig. 6, C and D). Anti-DNA antibodies develop in CD22-null mice after 9 mo of age, but glomerular immune complex deposits were not observed in these mice on a C57BL/6 background (45).

antibody (blue). FO, follicular compartment, and MZMM, MZ metallophilic macrophages. Results are representative of three mice per group in the age range of 8–12 wk. Bars, 100 µm. (B) Flow cytometric analyses reveal a reduction in MZ B cells in *Siae*$^{\Delta 2/\Delta 2}$ mice. Splenic B cell populations were analyzed by flow cytometry in mutant and WT mice. MZ, MZ B cells, NF, newly formed B cells; FO-I, follicular type I B cells and FO-II, follicular type II B cells (61). Results are representative of >10 mice per group. (C) Perisinusoidal BM B cells are reduced in *Siae*$^{\Delta 2/\Delta 2}$ mice as demonstrated by flow cytometry. BM B cell populations were analyzed by flow cytometry. Fractions (Fr.) A–C' represent pro–B and large pre–B cells, Fraction D represents small pre–B cells, Fraction E represents immature B cells, and Fraction F represents recirculating perisinusoidal B cells. The gating strategy was described previously (32). Results are representative of five mice per group. (D) Peritoneal B-1b B cells are increased in *Siae*$^{\Delta 2/\Delta 2}$ mice but B-1a B cells are decreased. Flow cytometric analyses were performed on peritoneal cavity B cells. Results are representative of five mice per group. The histogram shows absolute numbers of peritoneal B1 cells in WT and *Siae*$^{\Delta 2/\Delta 2}$ mice with three mice per group. Error bars represent SEM. (E) Siae affects B cell development in a B cell–intrinsic manner. *Rag-1*$^{-/-}$ mice were reconstituted with mutant or WT BM. Spleen and BM B cells were analyzed 7 wk later in the reconstituted mice. Results are representative of three mice per group. (F) Normal T cell development in the thymus and spleen in *Siae*$^{\Delta 2/\Delta 2}$ mice. Thymocyte and splenic populations were analyzed by flow cytometry in WT and *Siae*$^{\Delta 2/\Delta 2}$ mice. Results are representative of three mice per group.

Table I. Absolute numbers of B cells in spleen

Fraction	C57BL/6*	*Siae*$^{\Delta 2/\Delta 2}$*	Decrease (fold)
MZ	4.6 (0.9)	0.2 (0.1)	23.0
NF	2.9 (0.1)	1.8 (0.1)	1.6
MZP	2.1 (0.1)	0.2 (0.1)	10.5
FO	18.5 (1.5)	3.6 (1.1)	5.1
Total cell count	73.0 (3.8)	30.0 (6.3)	2.4

The various B cell populations (MZ, MZP, NF, FO, and Fractions A–F) are defined in the Fig. 5 legend. *, mean (SD) × 10^6; $n = 3$ mice per group.

Table II. Absolute numbers of B cells in BM

Fraction	C57BL/6	*Siae*$^{\Delta 2/\Delta 2}$		Decrease (fold)
A–C′	0.7 (0.1)	0.7 (0.3)	-	
D–F	2.4 (0.1)	2.5 (1.2)	-	
D	0.95 (0.1)	1.7 (1.0)	-	
E	0.2 (0.0)	0.3 (0.1)	-	
F	0.9 (0.1)	0.2 (0.1)		4.5
Total cell count	15.4 (3.7)*	16.9 (2.8)*	-	

*, mean (SD) × 10^6; $n = 3$ mice per group.

Table III. Absolute numbers of T cells in thymus

Fraction	C57BL/6	*Siae*$^{\Delta 2/\Delta 2}$	Decrease (fold)
CD4	1.9 (0.0)	1.6 (0.2)	1.18
CD8	0.8 (0.0)	1.5 (0.1)	-
Total cell count	39.5 (0.7)*	36.6 (1.5)*	1.07

*, mean (SD) × 10^6; $n = 3$ mice per group.

Table IV. Absolute numbers of T cells in spleen

Fraction	C57BL/6	*Siae*$^{\Delta 2/\Delta 2}$	Decrease (fold)
CD4	11.8 (0.2)	6.5 (0.6)	1.8
CD8	11.4 (1.2)	7.9 (0.2)	1.4

*, mean (SD) × 10^6; $n = 3$ mice per group.

It has been suggested that CD22 may function as an enforcer of peripheral tolerance (45), and a possible role for CD22 in setting signaling thresholds in the context of tolerance has been previously postulated (46). Lyn-null mice (17–19), as well as conditional SHP-1 mice (21), develop a lupuslike phenotype, supporting the notion that CD22, possibly other Siglecs, SHP-1, and Lyn are part of an inhibitory axis setting higher thresholds for B cell activation by self-antigens as well as by exogenous antigens (46). Siae may be an important component of this inhibitory axis (Fig. 7).

DISCUSSION

In this article, we show that mice with an engineered deletion in *Siae* phenocopy many of the alterations seen in CD22 -null mice (13–16). These common features include an enhancement of BCR-induced release of calcium from internal stores, the loss of MZ B cells, a reduction in BM perisinusoidal B cells, alterations in B cell proliferation that are dependent on the degree and duration of BCR cross-linking, some increase in follicular B cell apoptosis, and the spontaneous development of antinuclear antibodies.

Our results suggest that in *Siae* mutant mice, terminal α2–6-linked sialic acid moieties on *N*-linked glycans are 9-*O*-acetylated and, as a result, CD22 cannot readily inhibit BCR signaling. Although these results imply that ligation of CD22 by α2–6 sialic acid–containing ligands contributes to inhibitory signaling, the precise role that sialoglyconjugates play in the function of CD22 remains to be determined with certainty. The phenotypes of CD22 KO mice clearly suggest that a major in vivo function of this Siglec is to attenuate BCR signaling, but other studies have suggested that CD22 may potentially contribute to both inhibitory and activating functions (47). Mutating or blocking the sialic acid binding site of CD22 in a cell line context led to a loss of CD22

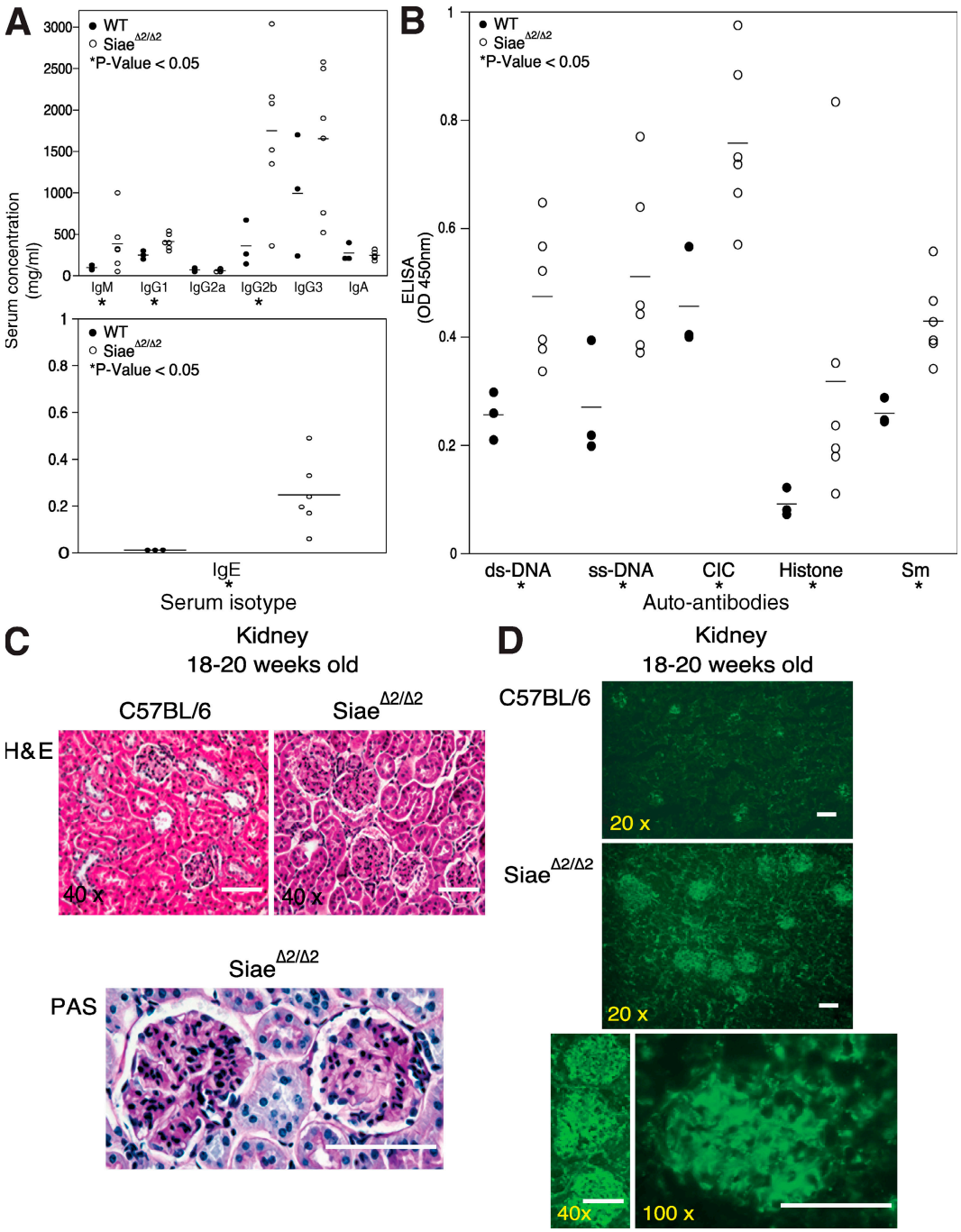

Figure 6. Increased serum immunoglobulins and autoantibodies in Siae mutant mice. (A) Serum immunoglobulins of specific isotypes are increased in mutant mice. Immunoglobulin isotypes were quantitated by ELISA. Each data point represents a single mouse. Horizontal bars represent the mean. (B) Increased levels of autoantibodies in the serum of *Siae*$^{\Delta 2/\Delta 2}$ mice. ELISA was used to estimate the levels of various autoimmune antibodies in serum. Each data point represents one mouse. Horizontal bars represent the mean. Ages of mice in A and B ranged from 20–60 wk. The results presented A and B and in C and D are all from the same set of mice. (C) Siae mutant mice show histological features of glomerulonephritis. Paraffin-embedded sections of kidney from mutant and WT mice were stained with hematoxylin and eosin (top) and with periodic acid Schiff (PAS) reagent (bottom). The glomeruli of the mutant mice (top right) show mesangial hypercellularity and expansion caused by periodic acid Schiff–positive deposits (bottom). The magnification is marked on each image. Bars, 100 µm. Results are representative of mice described in A and B. (D) IgG immune complex deposition in glomeruli of *Siae*$^{\Delta 2/\Delta 2}$ mice. Immunofluorescence studies on frozen sections of kidney reveal enlarged glomeruli with IgG-positive deposits in the mesangium in *Siae*$^{\Delta 2/\Delta 2}$ mice. The magnification is marked on each image. Bars, 100 µm. These sections are from the same mice as those shown in C.

inhibitory signaling as indicated by an enhanced calcium flux after BCR ligation (11, 48). Knockin mice harboring an identical mutation in the sialic acid binding site of CD22 exhibited some, but not all, of the phenotypic changes seen in CD22 null mice. Strikingly, an enhanced calcium flux was not observed in this knockin mouse after BCR ligation (22). Background-dependent modifier genes do contribute to differences seen in CD22-dependent phenotypes in KO and knockin animals, and there is growing evidence from SNP genotyping that even inbred mice strains are heterogenous at several loci (49). Nevertheless, no satisfactory explanation can be provided at present for the discrepant results of site directed mutagenesis-based studies of CD22 function.

ST6GalI is the sialyl transferase that transfers sialic acid in an α2–6-linked form from CMP-Sia to the preterminal galactose on *N*-glycans in the Golgi. In mice lacking ST6GalI, the absence of ligands for CD22 might have been expected to result in enhanced BCR signaling. Instead, these mice exhibit a gross defect in B cell signaling after ligation of the BCR and of other mitogenic receptors in B cells (37). One interpretation provided for these data is that in the absence of α2–6-linked sialic acid in the *ST6GalI*-null mouse, CD22 fails to multimerize and cannot be sequestered from the BCR (50). It is possible that in the absence of ST6GalI, inhibition of the BCR by CD22 is enhanced because of an abnormal facilitation of CD22 and IgM colocalization (23). However, the basis for this enhanced colocalization is not known, the reason for the relatively broad defect in signaling in *ST6GalI* mutant mice is not entirely clear, and is it not fully understood why these mice have defects in thymocyte development (38).

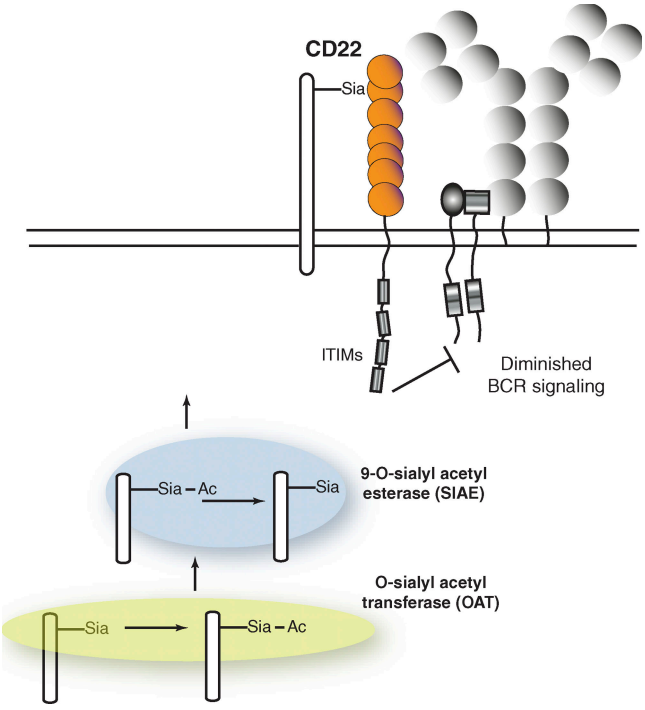

Figure 7. Siae regulates the availability of Siglec ligands on B cells and thus controls B cell antigen receptor signal strength. In mature B cells, BCR signaling thresholds are set by inhibitory molecules such as CD22. Sialic acid–containing ligands for Siglecs can be *O*-acetylated by an *O*-acetyltransferase in the Golgi. Acetyl moieties may be subsequently removed by Siae in an exocytic compartment or on the cell surface. In the absence of functional Siae, BCR signaling is no longer constrained by CD22 or other Siglecs on B cells.

Mice that lack both CD22 and ST6GalI exhibit enhanced BCR signaling similar to that seen in CD22-null mice (23, 51). Although these data have been interpreted to indicate a restoration in the absence of CD22 of BCR signaling that was diminished in the absence of ST6Gal I, both studies on $cd22^{-/-}/ST6GalI^{-/-}$ mice do not actually show a restoration of BCR signaling to WT levels but demonstrate that BCR signaling is enhanced in double mutant mice to levels similar to those seen in $cd22^{-/-}$ B cells. The loss of CD22 may be considered to be dominant. These data are therefore compatible with the possibility that CD22 can provide inhibitory signals constitutively, presumably by providing ITIM tyrosines as a potential substrate for phosphorylation by Lyn and other Src family kinases. Nevertheless, CD22 might provide optimal inhibitory signals only in the presence of its sialoglycoconjugate ligands. The total absence of α2–6-linked sialic acid may represent a relatively drastic alteration that could result in aberrant capping of *N*-acetyllactosamine termini of many glycans (52) and might affect B cell function adversely in poorly understood ways. A subtle alteration of the structure of CD22 ligands, such as enhanced 9-*O*-acetylation of sialic acid in mice with mutant *Siae*, or the combined loss of Neu5Gc and enhanced 9-*O*-acetylation of sialic acid in the *Cmah*-null mouse and the *Cmah-Siae* double mutant mouse both appear to provide somewhat different insights compared with those obtained from the *ST6Gal1* KO mouse harboring a more global alteration in CD22 ligand structure.

In contrast to *Siae* mutant mice that have detectable anti-DNA antibodies when they are 5 mo of age, $cd22^{-/-}$ mice, also on a C57BL/6 background, develop anti-DNA antibodies only when they are at least 9 mo old, and these latter mice do not develop kidney deposits of antibody and complement (45). Collectively, the spontaneous secretion of increased levels of class switched immunoglobulins and antichromatin antibodies, the accumulation of glomerular immune complex deposits, and the apparent activation-dependent attrition of follicular B cells in *Siae* mutant mice suggest a stronger phenotype in these mice than that observed in mice lacking CD22. These data suggest indirectly that Siae might not only attenuate CD22 function but may also possibly regulate an additional Siglec or Siglecs in B cells, although direct evidence for such a hypothesis is lacking. A second inhibitory Siglec in murine B cells, Siglec G, has been previously described (53). However, although Siglec G–deficient mice exhibit a marked increase in B-1a B cells, IgG autoantibodies are not increased. It remains to be determined whether this or any other Siglec, other than CD22, is regulated by Siae. It also remains to be determined if an engineered defect in *Cmah* leads to an autoimmune state.

It has been previously suggested that CD22, Lyn, and SHP-1 set a threshold for B cell activation (46). The enhanced

BCR signaling noted in mice that lack CD22 and in *Siae* mutant mice suggests that loss of tolerance may result from a mechanism that is distinct from models invoking clonal deletion, receptor editing, and anergy, all of which might be presumed to be enhanced, not abrogated, by an increase in BCR signal strength in B cells. These well established mechanisms of tolerance have been studied extensively using transgenic and knockin models that use relatively high-affinity BCRs for model self-antigens. The analysis of anti–HEL-soluble HEL double transgenic mice in a *cd22*-null background did not result in a break in tolerance to HEL (46, 54). We expand here on a suggestion originally made by Neuberger and coworkers (45) and also discussed by Cornall et al. (46) that CD22, and possibly other Siglecs, might set thresholds for the activation of B cells in the periphery. Weakly self-reactive B cells may not be activated by self-antigens because CD22 helps set an activation threshold in the periphery. If the strength of activation of B cells by self-antigens were to cross a threshold, the processing and presentation of self-antigens could be facilitated, and the unwanted entry of relatively weakly self-reactive B cells into the germinal center reaction might also occur. There are many potential ways in which, during an infection, a self-structure may be physically complexed with a foreign protein. In a viral infection, for instance, host chromatin may contain proteins of viral origin bound to host antigens including host nucleic acids. If the BCR threshold signaling is not set high enough (because of defects in CD22 or Siae for instance), self-antigens might not only activate weakly self-reactive B cells but may also deliver physically linked foreign proteins to endosomes in B cells, thus permitting the receipt of T cell help for somatic mutation. It is perhaps significant that in human autoimmune diseases in which antibodies are known to be relevant, pathogenic autoantibodies tend to be somatically mutated and class switched. Siglecs, assisted by Siae, presumably play a key role in keeping weakly self-reactive B cells quiescent. It is clear that analyses of responses to one specific T cell–dependent synthetic immunogen are not apparently consonant with the spontaneous immunoglobulin and autoantibody levels observed in *Siae* mutant mice, and there is a need for more detailed immunization studies in these mutant mice and in controls.

Elucidating the full complexity of the biological functions of 9-*O*-acetylation of sialic acid will require the analysis of a mutant organism that lacks the sialic acid *O*-acetyl transferase in the Golgi complex that can transfer an acetyl moiety from acetyl CoA to the 7-OH or 9-OH position of terminal sialic acid residue on glycoconjugates. Although more than one sialic acid *O*-acetyl transferase may exist (55), to date no such O-acetyl transferase has been molecularly identified. Our data indicate that modulation of 9-*O*-acetylation of sialic acid, a modification which was first described more than half a century ago (1), regulates inhibitory signaling in B lymphocytes and participates in the maintenance of immunological tolerance. Furthermore, our ongoing unpublished studies involving deep resequencing of the *SIAE* gene in human controls, and patients with autoimmunity have revealed a strong association of rare loss-of-function variants of *SIAE* with autoimmune disease, suggesting that the regulatory function of Siae is not restricted to rodents (unpublished data).

Siae was identified over a decade ago as a gene that is regulated during B cell development (26). We have now shown that this enzyme regulates the cell surface acetylation of sialic acid. It remains to be determined where exactly in B cells Siae is located and whether the expression and catalytic activity of this enzyme is regulated during antigen-mediated B cell activation.

MATERIALS AND METHODS

Mice. 8–12-wk-old C57BL/6 and B6.129S7-*Rag1* mice (The Jackson Laboratory) were used in this study. Animal procedures were approved by the subcommittees on research animal care at Massachussetts General Hospital and at the University of California, San Diego.

Generation of homozygous *Siae*$^{\Delta 2/\Delta 2}$ mice. Exon 2 of *Siae* encoding the N terminus of the Lse form of Siae was deleted. The Siae targeting vector was assembled from a 129/Sv genomic clone by inserting the 0.7-kb BamHI–XbaI fragment, containing exon 2 of Siae, into the BamHI site of the pflox vector (56). Adjacent 129/Sv Siae genomic sequences were added by subcloning the 1.5-kb XbaI–NheI fragment into the XhoI site and the BamHI–BamHI 9-kb fragment into the SalI site of pflox. 10 μg of NotI-linearized targeting vector was electroporated into 150 μg/ml R1 ES cells and G418-resistant transfectants, which was positive by PCR for homologous recombination and retaining all three loxP sites, and was transfected with the pCreHygro expression vector. After 4 d of 2-μM gancyclovir selection, subclones were isolated and those harboring the *Siae*-floxed allele were detected by Southern blotting with BamHI–SpeI genomic digestion and a loxP probe. Two ES cell clones were used to generate chimeric mice in C57BL/6 host embryos. Offspring were genotyped by Southern blotting with BamHI–SpeI tail DNA hybridized to the 3′ probe (3S0.6). Heterozygous offspring were mated to C57BL/6 ZP3-Cre mice. Female offspring were then mated to produce homozygous *Siae*$^{\Delta 2/\Delta 2}$ mice. PCR primers used for genotyping were as follows: PS-LseG-16, 5′-TTTAGGAGCAAGGGGTTGGCCAAGA-3′; PS-LseG-B, 5′-GGTTTCCTGACCTTGGCACAAGGT-3′; and LOX-R, 5′-CGGTACCCGGGGATCAATTCGAG-3′. PS-LseG-16 and PS-LseG-B yield the 420-bp WT band and PS-LseG-16 and LOX-R the 340-bp mutant band. The mice used in these studies were backcrossed into the C57BL/6 background for 10 generations and then maintained by intercrossing.

Antibodies, staining, and flow cytometry. The following murine monoclonal antibody conjugates were used: Allophycocyanin (APC)-RA3-6B2 (anti-CD45R/B220, rat IgG_{2a}, κ), FITC-S7 (anti-CD43, rat IgG_{2a}, κ), FITC-7G6 (anti-CD21/CD35, rat IgG_{2b}), FITC-Cy34.1 (anti-CD22.2, mouse [DBA/1] IgG_1, κ), APC-53-7.3 (anti-CD5, rat IgG_{2a}, κ), APC-M1/70 (anti-CD11b, rat IgG_{2b}, κ), r-phycoerythrin (R-PE)-GK1.5 (anti-CD4, rat IgG_{2b}, κ), and FITC-53-6.7 (anti-CD8a, rat IgG_{2a},κ; all from BD); and APC and R-PE-1B4B1 (anti-IgM, rat IgG), and R-PE-11-26 (anti-IgD, rat IgG_{2a}, κ; SouthernBiotech).

Single cell suspensions were made from spleen, BM (one femur and tibia), thymus, and peritoneal washings using standard methodology. Red cells were lysed with 2 ml ACK lysing buffer (Cambrex). The lysis buffer was neutralized by adding 10 ml PBS and 0.2% BSA (PBA). Before staining, 1×10^6 cells were reacted with 2.5 μg of 2.4G2 (anti-CD16/CD32 [Fcγ III/II receptor], rat IgG_{2b}, κ; BD). Surface staining was performed using appropriate dilutions of antibodies in 12 × 75-mm round-bottom polystyrene tubes in a volume of 200 μl for 30 min in the dark at 4°C.

Flow cytometric analysis was performed as previously described (57) on a dual laser FC500 (Beckman Coulter), a MoFlo (Dako), and a FACSAria (BD). Unstained cells were used to set voltage and single color positive controls were used for electronic compensation. Viable cells were determined by forward and side scatter characteristics and 3–5 × 10^4 gated events were collected. Gates were set as previously described (33). Processed samples were

analyzed using RXP (Beckman Coulter), and FloJo v8.8 (Tree Star, Inc.) analysis software.

Reconstitution of the lymphoid compartment in Rag-1–deficient mice. *Rag-1*$^{-/-}$ mice were irradiated with 7.5 Gy and reconstituted with 5×10^6 WT or mutant adult BM cells via tail vein injection. Reconstitution of the BM and spleen was assessed 7 wk later by flow cytometry.

Detection of 9-*O*-acetylated sialic acid on splenocytes. The CHE-FcD probe, a fusion protein composed of the extracellular domains of the influenza C hemagglutinin esterase (CHE) which binds 9-*O*-acetylated sialic acids, and the Fc portion of human IgG_1(Fc), treated with diisopropylfluorophosphate (D) was generated as previously described (28, 58). The chimeric CHE Fc-D protein was precomplexed with Cy5 or FITC-F(ab′)$_2$ goat anti–human IgG (Jackson ImmunoResearch Laboratories; 1 µl of a 1:10 dilution of CHE-FcD in PBA with 2 µl of the secondary antibody in a total volume of 50 µl PBA) for 2 h at 4°C in the dark. 10^6 cells in 50 µl PBA were preincubated for 45 min at 37°C, added to the precomplex, and incubated on ice for an additional 1.5 h. The cells were washed once, reacted with 2.4G2, an Fcγ III/II receptor-blocking antibody, and surface stained as described earlier. Staining of acetylated sialic acid on CD4$^+$ T cells served as a positive control (28).

BCR cross-linking and accumulation of cytosolic calcium. In brief, Indo-1 AM (acetoxymethyl ester; Invitrogen) was added to 3×10^6 splenocytes in 500 µl HBSS (Invitrogen) and 10% FCS (HBSS-10). The final concentration of Indo-1 was 1 µM. The cells were incubated in a 37°C water bath for 30 min, held at room temperature for 5 min, and washed with HBSS containing 2 mM Hepes buffer and no serum (HBSH-0). All manipulations including the incubation were in the dark. Cells were then reacted with 2.4G2, an Fcγ III/II receptor-blocking antibody, surface stained as described earlier, and washed with HBSH-0, all in the dark at 4°C. The cells were resuspended in the residual volume and an additional 50 µl HBSH-0 was added to make a total volume of ∼150 µl. The cells were then split into three 50-µl aliquots and the volume made up to 100 µl with HBSH-0. The cells were held in the dark at 4°C before analysis. Before calcium flux measurements, the cells were filtered and incubated at RT for 10 min. The cells were warmed to 37°C in a heat block for 6 min and placed in the flow cytometer in a chamber maintained at 37°C. After a flow rate of ∼500 cells/s was established, acquisition was begun to record a 30-s baseline. After addition of stimulatory antibody (Fab_2 fragments of anti-IgM), acquisition was continued for another 180 s with the cells at 37°C. Between samples, distilled water was run at a high flow rate for 2 min to flush the lines. The flow cytometer used was a FACS Vantage SE (BD) operating with a laser (Innova Enterprise Model 621; Coherent, Inc.).

Serum immunoglobulins and autoantibodies. Total serum immunoglobulins of various isotypes were analyzed using an ELISA approach (Alpha Diagnostic International, San Antonio, TX). ELISA was also used to quantify serum autoantibodies (anti-dsDNA, anti-ssDNA, anti-histone, anti-Sm) and circulating immune complexes (all from Alpha Diagnostic).

Immunofluorescence staining, immunohistochemistry and histological staining. Immunofluorescence was performed as previously described (59) with some modifications. Sections for immunofluorescence were blocked with 20% normal goat serum in 1% BSA/PBS for 20 min and stained with FITC-AffiniPure F(ab′)$_2$ goat anti–mouse IgG (H + L; Jackson ImmunoResearch Laboratories) diluted 1:200 in 5% normal goat serum/1% BSA/PBS for 15 min in the dark at room temperature. After rinsing three times in PBS for 5′ each, sections were mounted using 25 µl of Vectashield (Vector Laboratories). Immunohistochemistry was performed as described previously (60). Paraffin sections were stained with hematoxylin and eosin and the periodic acid Schiff reagent using standard methods.

Immunoprecipitation and Western blot analysis. The method used by Poe et al. (22) was adhered to with some modifications. 10^7 murine splenocytes or sorted 5×10^5 B cells were lysed before and after BCR ligation using 1% NP40 in PBS. Lysates were immunoprecipitated using anti-CD22 (CD-22 rabbit IgG; Epitomics, Inc.) and protein A Sepharose, and after separation on an SDS/polyacrylamide gel and Western transfer, membranes were probed with antibodies to CD22, SHP-1, and phosphotyrosine (anti-CD22.2, clone Lyb-8.2 [BD]; anti-SHP1/2 rabbit polyclonal IgG, and antiphosphotyrosine, clone 4G10 [Millipore]). Relative expression of CD22 and SHP-1 was quantified using Quantity One software (Bio-Rad Laboratories).

Online supplemental material. Fig. S1 shows that Siae is secreted from stably transfected U2OS cells. Fig. S2 shows that Siae is expressed on the surface of transfected U2OS cells and is also partially present in lysosomes. Fig. S3 shows the presence of truncated *Siae* mRNA in mutant mice as revealed by RT-PCR. Fig. S4 shows accelerated and enhanced BCR-induced calcium release in purified B lymphocytes from *Siae* mutant mice. Figs. S5 and S6 show that surface expression of CD22 on splenocytes in *Siae*$^{\Delta 2/\Delta 2}$ mice is unaltered compared with WT mice. Fig. S7 shows that Siae mutant splenocytes proliferate more than WT B cells. Fig. S8 shows a stimulus strength–dependent inhibition of B cell proliferation after BCR cross-linking. In Fig. S9, mutant resting B splenocytes show a mild increase in apoptosis. In Fig. S10, peripheral B cell populations and the response to BCR cross-linking of the *Cmah*-null mouse are depicted, and in Fig. S11, similar studies are presented that were performed on *Siae*/*Cmah* double mutant mice. Fig. S12 shows antibody responses to synthetic T cell–dependent and T cell–independent antigens in *Siae* mutant and WT mice. Online supplemental material is available at http://www.jem.org/cgi/content/full/jem.20081399/DC1.

We acknowledge initial studies of the mouse phenotype by Dawne Page, Jamey Marth, and Laura Martin. Joanne Yetz-Aldape, Suzan Lazo-Kallanian, and John Daley are thanked for help with flow cytometry. We thank Eveline Schneeberger for advice on renal pathology. We thank Stacey Beganny and Jonathan Foley for help with densitometry, and Emily Forbes and Johnathan Whetstine for help with confocal microscopy.

These studies were supported by grants from the National Institutes of Health to S. Pillai (AI064930 and AI069458) and A. Varki (GM32373 and P01HL057345).

The authors have no conflicting financial interests.

Submitted: 30 June 2008
Accepted: 1 December 2008

REFERENCES

1. Schauer, R. 2000. Achievements and challenges of sialic acid research. *Glycoconj. J.* 17:485–499.
2. Angata, T., and A. Varki. 2002. Chemical diversity in the sialic acids and related alpha-keto acids: an evolutionary perspective. *Chem. Rev.* 102:439–469.
3. Herrler, G., R. Rott, H.D. Klenk, H.P. Muller, A.K. Shukla, and R. Schauer. 1985. The receptor-destroying enzyme of influenza C virus is neuraminate-O-acetylesterase. *EMBO J.* 4:1503–1506.
4. Vlasak, R., W. Luytjes, W. Spaan, and P. Palese. 1988. Human and bovine coronaviruses recognize sialic acid-containing receptors similar to those of influenza C viruses. *Proc. Natl. Acad. Sci. USA.* 85:4526–4529.
5. Varki, A., F. Hooshmand, S. Diaz, N.M. Varki, and S.M. Hedrick. 1991. Developmental abnormalities in transgenic mice expressing a sialic acid-specific 9-O-acetylesterase. *Cell.* 65:65–74.
6. Sjoberg, E.R., L.D. Powell, A. Klein, and A. Varki. 1994. Natural ligands of the B cell adhesion molecule CD22β can be masked by 9-*O*-acetylation of sialic acids. *J. Cell Biol.* 126:549–562.
7. Varki, A. 2007. Glycan-based interactions involving vertebrate sialic-acid-recognizing proteins. *Nature.* 446:1023–1029.
8. Crocker, P.R., J.C. Paulson, and A. Varki. 2007. Siglecs and their roles in the immune system. *Nat. Rev. Immunol.* 7:255–266.
9. Crocker, P.R. 2002. Siglecs: sialic-acid-binding immunoglobulin-like lectins in cell-cell interactions and signalling. *Curr. Opin. Struct. Biol.* 12:609–615.
10. Powell, L.D., D. Sgroi, E.R. Sjoberg, I. Stamenkovic, and A. Varki. 1993. Natural ligands of the B cell adhesion molecule CD22 beta carry N-linked oligosaccharides with alpha-2,6-linked sialic acids that are required for recognition. *J. Biol. Chem.* 268:7019–7027.

11. Jin, L., P.A. McLean, B.G. Neel, and H.H. Wortis. 2002. Sialic acid binding domains of CD22 are required for negative regulation of B cell receptor signaling. *J. Exp. Med.* 195:1199–1205.
12. Doody, G.M., L.B. Justement, C.C. Delibrias, R.J. Matthews, J. Lin, M.L. Thomas, and D.T. Fearon. 1995. A role in B cell activation for CD22 and the protein tyrosine phosphatase SHP. *Science.* 269:242–244.
13. O'Keefe, T.L., G.T. Williams, S.L. Davies, and M.S. Neuberger. 1996. Hyperresponsive B cells in CD22-deficient mice. *Science.* 274:798–801.
14. Otipoby, K.L., K.B. Andersson, K.E. Draves, S.J. Klaus, A.G. Farr, J.D. Kerner, R.M. Perlmutter, C.L. Law, and E.A. Clark. 1996. CD22 regulates thymus-independent responses and the lifespan of B cells. *Nature.* 384:634–637.
15. Sato, S., A.S. Miller, M. Inaoki, C.B. Bock, P.J. Jansen, M.L. Tang, and T.F. Tedder. 1996. CD22 is both a positive and negative regulator of B lymphocyte antigen receptor signal transduction: altered signaling in CD22-deficient mice. *Immunity.* 5:551–562.
16. Nitschke, L., R. Carsetti, B. Ocker, G. Kohler, and M.C. Lamers. 1997. CD22 is a negative regulator of B-cell receptor signalling. *Curr. Biol.* 7:133–143.
17. Hibbs, M.L., D.M. Tarlinton, J. Armes, D. Grail, G. Hodgson, R. Maglitto, S.A. Stacker, and A.R. Dunn. 1995. Multiple defects in the immune system of Lyn-deficient mice, culminating in autoimmune disease. *Cell.* 83:301–311.
18. Nishizumi, H., I. Taniuchi, Y. Yamanashi, D. Kitamura, D. Ilic, S. Mori, T. Watanabe, and T. Yamamoto. 1995. Impaired proliferation of peripheral B cells and indication of autoimmune disease in lyn-deficient mice. *Immunity.* 3:549–560.
19. Chan, V.W., F. Meng, P. Soriano, A.L. DeFranco, and C.A. Lowell. 1997. Characterization of the B lymphocyte populations in Lyn-deficient mice and the role of Lyn in signal initiation and down-regulation. *Immunity.* 7:69–81.
20. Cyster, J.G., and C.C. Goodnow. 1995. Protein tyrosine phosphatase 1C negatively regulates antigen receptor signaling in B lymphocytes and determines thresholds for negative selection. *Immunity.* 2:13–24.
21. Pao, L.I., K.P. Lam, J.M. Henderson, J.L. Kutok, M. Alimzhanov, L. Nitschke, M.L. Thomas, B.G. Neel, and K. Rajewsky. 2007. B cell-specific deletion of protein-tyrosine phosphatase Shp1 promotes B-1a cell development and causes systemic autoimmunity. *Immunity.* 27:35–48.
22. Poe, J.C., Y. Fujimoto, M. Hasegawa, K.M. Haas, A.S. Miller, I.G. Sanford, C.B. Bock, M. Fujimoto, and T.F. Tedder. 2004. CD22 regulates B lymphocyte function in vivo through both ligand-dependent and ligand-independent mechanisms. *Nat. Immunol.* 5:1078–1087.
23. Collins, B.E., B.A. Smith, P. Bengtson, and J.C. Paulson. 2006. Ablation of CD22 in ligand-deficient mice restores B cell receptor signaling. *Nat. Immunol.* 7:199–206.
24. Walker, J.A., and K.G. Smith. 2008. CD22: an inhibitory enigma. *Immunology.* 123:314–325.
25. Guimaraes, M.J., J.F. Bazan, J. Castagnola, S. Diaz, N.G. Copeland, D.J. Gilbert, N.A. Jenkins, A. Varki, and A. Zlotnik. 1996. Molecular cloning and characterization of lysosomal sialic acid O-acetylesterase. *J. Biol. Chem.* 271:13697–13705.
26. Stoddart, A., Y. Zhang, and C.J. Paige. 1996. Molecular cloning of the cDNA encoding a murine sialic acid-specific 9-O-acetylesterase and RNA expression in cells of hematopoietic and non-hematopoietic origin. *Nucleic Acids Res.* 24:4003–4008.
27. Takematsu, H., S. Diaz, A. Stoddart, Y. Zhang, and A. Varki. 1999. Lysosomal and cytosolic sialic acid 9-O-acetylesterase activities can be encoded by one gene via differential usage of a signal peptide-encoding exon at the N terminus. *J. Biol. Chem.* 274:25623–25631.
28. Krishna, M., and A. Varki. 1997. 9-*O*-Acetylation of sialomucins: a novel marker of murine CD4 T cells that is regulated during maturation and activation. *J. Exp. Med.* 185:1997–2013.
29. Cariappa, A., M. Tang, C. Parng, E. Nebelitskiy, M. Carroll, K. Georgopoulos, and S. Pillai. 2001. The follicular versus marginal zone B lymphocyte cell fate decision is regulated by Aiolos, Btk, and CD21. *Immunity.* 14:603–615.
30. Samardzic, T., D. Marinkovic, C.P. Danzer, J. Gerlach, L. Nitschke, and T. Wirth. 2002. Reduction of marginal zone B cells in CD22-deficient mice. *Eur. J. Immunol.* 32:561–567.
31. Pillai, S., A. Cariappa, and S.T. Moran. 2005. Marginal Zone B Cells. *Annu. Rev. Immunol.* 23:161–196.
32. Cariappa, A., I.B. Mazo, C. Chase, H.N. Shi, H. Liu, Q. Li, H. Rose, H. Leung, B.J. Cherayil, P. Russell, et al. 2005. Perisinusoidal B cells in the bone marrow participate in T-independent responses to blood-borne microbes. *Immunity.* 23:397–407.
33. Cariappa, A., C. Chase, H. Liu, P. Russell, and S. Pillai. 2007. Naive recirculating B cells mature simultaneously in the spleen and bone marrow. *Blood.* 109:2339–2345.
34. Wang, J.H., N. Avitahl, A. Cariappa, C. Friedrich, T. Ikeda, A. Renold, K. Andrikopoulos, L. Liang, S. Pillai, B.A. Morgan, and K. Georgopoulos. 1998. Aiolos regulates B cell activation and maturation to effector state. *Immunity.* 9:543–554.
35. Pan, C., N. Baumgarth, and J.R. Parnes. 1999. CD72-deficient mice reveal nonredundant roles of CD72 in B cell development and activation. *Immunity.* 11:495–506.
36. Ngo, V.N., R.J. Cornall, and J.G. Cyster. 2001. Splenic T zone development is B cell dependent. *J. Exp. Med.* 194:1649–1660.
37. Hennet, T., D. Chui, J.C. Paulson, and J.D. Marth. 1998. Immune regulation by the ST6Gal sialyltransferase. *Proc. Natl. Acad. Sci. USA.* 95:4504–4509.
38. Marino, J.H., C. Tan, B. Davis, E.S. Han, M. Hickey, R. Naukam, A. Taylor, K.S. Miller, C.J. Van De Wiele, and T.K. Teague. 2008. Disruption of thymopoiesis in ST6Gal I-deficient mice. *Glycobiology.* 18:719–726.
39. Blixt, O., B.E. Collins, I.M. van den Nieuwenhof, P.R. Crocker, and J.C. Paulson. 2003. Sialoside specificity of the siglec family assessed using novel multivalent probes: identification of potent inhibitors of myelin-associated glycoprotein. *J. Biol. Chem.* 278:31007–31019.
40. Brinkman-Van der Linden, E.C., E.R. Sjoberg, L.R. Juneja, P.R. Crocker, N. Varki, and A. Varki. 2000. Loss of N-glycolylneuraminic acid in human evolution. Implications for sialic acid recognition by siglecs. *J. Biol. Chem.* 275:8633–8640.
41. Kelm, S., R. Brossmer, R. Isecke, H.J. Gross, K. Strenge, and R. Schauer. 1998. Functional groups of sialic acids involved in binding to siglecs (sialoadhesins) deduced from interactions with synthetic analogues. *Eur. J. Biochem.* 255:663–672.
42. Collins, B.E., O. Blixt, N.V. Bovin, C.P. Danzer, D. Chui, J.D. Marth, L. Nitschke, and J.C. Paulson. 2002. Constitutively unmasked CD22 on B cells of ST6Gal I knockout mice: novel sialoside probe for murine CD22. *Glycobiology.* 12:563–571.
43. Hedlund, M., P. Tangvoranuntakul, H. Takematsu, J.M. Long, G.D. Housley, Y. Kozutsumi, A. Suzuki, A. Wynshaw-Boris, A.F. Ryan, R.L. Gallo, et al. 2007. N-glycolylneuraminic acid deficiency in mice: implications for human biology and evolution. *Mol. Cell. Biol.* 27:4340–4346.
44. Naito, Y., H. Takematsu, S. Koyama, S. Miyake, H. Yamamoto, R. Fujinawa, M. Sugai, Y. Okuno, G. Tsujimoto, T. Yamaji, et al. 2007. Germinal center marker GL7 probes activation-dependent repression of N-glycolylneuraminic acid, a sialic acid species involved in the negative modulation of B-cell activation. *Mol. Cell. Biol.* 27:3008–3022.
45. O'Keefe, T.L., G.T. Williams, F.D. Batista, and M.S. Neuberger. 1999. Deficiency in CD22, a B cell–specific inhibitory receptor, is sufficient to predispose to development of high affinity autoantibodies. *J. Exp. Med.* 189:1307–1313.
46. Cornall, R.J., J.G. Cyster, M.L. Hibbs, A.R. Dunn, K.L. Otipoby, E.A. Clark, and C.C. Goodnow. 1998. Polygenic autoimmune traits: Lyn, CD22, and SHP-1 are limiting elements of a biochemical pathway regulating BCR signaling and selection. *Immunity.* 8:497–508.
47. Tedder, T.F., M. Inaoki, and S. Sato. 1997. The CD19-CD21 complex regulates signal transduction thresholds governing humoral immunity and autoimmunity. *Immunity.* 6:107–118.
48. Kelm, S., J. Gerlach, R. Brossmer, C.P. Danzer, and L. Nitschke. 2002. The ligand-binding domain of CD22 is needed for inhibition of the B cell receptor signal, as demonstrated by a novel human CD22-specific inhibitor compound. *J. Exp. Med.* 195:1207–1213.
49. Watkins-Chow, D.E., and W.J. Pavan. 2008. Genomic copy number and expression variation within the C57BL/6J inbred mouse strain. *Genome Res.* 18:60–66.

50. Han, S., B.E. Collins, P. Bengtson, and J.C. Paulson. 2005. Homomultimeric complexes of CD22 in B cells revealed by protein-glycan cross-linking. *Nat. Chem. Biol.* 1:93–97.
51. Ghosh, S., C. Bandulet, and L. Nitschke. 2006. Regulation of B cell development and B cell signalling by CD22 and its ligands alpha2,6-linked sialic acids. *Int. Immunol.* 18:603–611.
52. Martin, L.T., J.D. Marth, A. Varki, and N.M. Varki. 2002. Genetically altered mice with different sialyltransferase deficiencies show tissue-specific alterations in sialylation and sialic acid 9-O-acetylation. *J. Biol. Chem.* 277:32930–32938.
53. Hoffmann, A., S. Kerr, J. Jellusova, J. Zhang, F. Weisel, U. Wellmann, T.H. Winkler, B. Kneitz, P.R. Crocker, and L. Nitschke. 2007. Siglec-G is a B1 cell-inhibitory receptor that controls expansion and calcium signaling of the B1 cell population. *Nat. Immunol.* 8:695–704.
54. Ferry, H., T.L. Crockford, K. Silver, N. Rust, C.C. Goodnow, and R.J. Cornall. 2005. Analysis of Lyn/CD22 double-deficient B cells in vivo demonstrates Lyn- and CD22-independent pathways affecting BCR regulation and B cell survival. *Eur. J. Immunol.* 35:3655–3663.
55. Shi, W.X., R. Chammas, and A. Varki. 1998. Induction of sialic acid 9-O-acetylation by diverse gene products: implications for the expression cloning of sialic acid O-acetyltransferases. *Glycobiology.* 8:199–205.
56. Chui, D., M. Oh-Eda, Y.F. Liao, K. Panneerselvam, A. Lal, K.W. Marek, H.H. Freeze, K.W. Moremen, M.N. Fukuda, and J.D. Marth. 1997. Alpha-mannosidase-II deficiency results in dyserythropoiesis and unveils an alternate pathway in oligosaccharide biosynthesis. *Cell.* 90:157–167.
57. Cariappa, A., T.J. Kim, and S. Pillai. 1999. Accelerated emigration of B lymphocytes in the Xid mouse. *J. Immunol.* 162:4417–4423.
58. Martin, L.T., A. Verhagen, and A. Varki. 2003. Recombinant influenza C hemagglutinin-esterase as a probe for sialic acid 9-O-acetylation. *Methods Enzymol.* 363:489–498.
59. Cariappa, A., H.C. Liou, B.H. Horwitz, and S. Pillai. 2000. Nuclear factor κB is required for the development of marginal zone B lymphocytes. *J. Exp. Med.* 192:1175–1182.
60. Cariappa, A., T. Shoham, H. Liu, S. Levy, C. Boucheix, and S. Pillai. 2005. The CD9 tetraspanin is not required for the development of peripheral B cells or for humoral immunity. *J. Immunol.* 175: 2925–2930.
61. Cariappa, A., C. Boboila, S.T. Moran, H. Liu, H.N. Shi, and S. Pillai. 2007. The recirculating B cell pool contains two functionally distinct, long-lived, posttransitional, follicular B cell populations. *J. Immunol.* 179:2270–2281.